Utility of the inverse partial fluorescence for electronic structure studies of battery materials

H. Wadati,[1, 2, *] A. J. Achkar,[3] D. G. Hawthorn,[3] T. Z. Regier,[4] M. P. Singh,[5]
K. D. Truong,[5] P. Fournier,[5] G. Chen,[6] T. Mizokawa,[7] and G. A. Sawatzky[2]

[1]*Department of Applied Physics and Quantum-Phase Electronics Center (QPEC),*
University of Tokyo, Hongo, Tokyo 113-8656, Japan
[2]*Department of Physics and Astronomy, University of British Columbia, Vancouver, British Columbia V6T 1Z1, Canada*
[3]*Department of Physics and Astronomy, University of Waterloo, Waterloo, Ontario N2L 3G1, Canada*
[4]*Canadian Light Source, University of Saskatchewan, Saskatoon, Saskatchewan S7N 0X4, Canada*
[5]*Regroupement Québécois sur les Matériaux de Pointe et Département de Physique,*
Université de Sherbrooke, Sherbrooke, Québec J1K 2R1, Canada
[6]*College of Physics/State Key Laboratory of Superhard Materials,*
Jilin University, Changchun 130012, People's Republic of China
[7]*Department of Complexity Science and Engineering,*
University of Tokyo, Kashiwa, Chiba 277-8561, Japan
(Dated: January 5, 2012)

X-ray absorption spectroscopy (XAS) is one of the most widely used experimental techniques to study the electronic and spatial structure of materials. Fluorescence yield mode is bulk-sensitive, but has several serious problems coming from saturation effects. In this study, we show the usefulness of partial fluorescence yields in addressing these problems. We discuss the different behaviors of La_2NiMnO_6 and $LiMnO_2$ at the Mn $2p$ absorption edges. The total fluorescence yield produces misleading spectra for $LiMnO_2$ due to the absence of high-Z (Z: atomic number) elements. We conclude that the measurement of the inverse partial fluorescence yield is essential in studies of $LiMnO_2$, which is a hotly debated Li-ion battery material.

X-ray absorption spectroscopy (XAS) is an experimental probe of the electronic and spatial structure of materials and is widely used in various fields of the natural sciences [1–3]. XAS is the measurement of photo-absorption by excitation of a core electron into the unoccupied states as a function of photon energy. There are three measurement modes for XAS, the transmission mode, the electron yield (EY) mode, and the fluorescence yield (FY) mode. In the transmission mode, the intensity of the x-rays is measured in front of and behind the sample and the ratio of the transmitted x-rays is determined. Transmission mode experiments are standard for hard x-rays, while for soft x-rays they are difficult to perform due to the strong interaction of soft x-rays with the sample. An alternative to the transmission mode experiment has been provided by measuring the decay products of the core holes which are created in the absorption process. The decay products include electrons, photons, and ions escaping from the surface of the sample. The yield modes can be classified into the EY mode and the FY mode. The total electron yield (TEY) is the most widely used detection technique. The energy of the outgoing electrons is not selected and simply all the escaping electrons are counted. The signal is dominated by secondary electrons which are created in the cascade process of the Auger decay electrons. The estimated probing depth of this technique using soft x-rays is ~ 40 Å. Besides the EY mode, the fluorescent decay of the core hole can be also used for XAS measurements. In the FY mode, the photons created in the fluorescent process have a mean free path of the same order of magnitude as the incident

x-rays. Consequently, the FY mode has a large probing depth (> 1000 Å in the soft x-ray region), and is particularly suitable for studying bulk electronic structures. The FY measurements can be performed by either the total fluorescence yield (TFY) or the partial fluorescence yield (PFY). In the TFY mode photons with any energy are counted, whereas the PFY mode uses an energy-sensitive detector and selects photons within a particular range of energies.

$$
\begin{aligned}
\mathrm{TFY} &= \mathrm{PFY_{Mn}} + \sum_X \mathrm{PFY_{other}} \\
&= C(E_f)\frac{\omega_{\mathrm{Mn}}(E_i, E_{\mathrm{Mn}})\mu_{\mathrm{Mn}}(E_i)}{\mu_T(E_i) + \mu_T(E_{\mathrm{Mn}})\frac{\sin\alpha}{\sin\beta}} \\
&\quad + C(E_f)\sum_X \frac{\omega_X(E_i, E_X)\mu_X(E_i)}{\mu_T(E_i) + \mu_T(E_X)\frac{\sin\alpha}{\sin\beta}},
\end{aligned}
\tag{1}
$$

where

$$
\mu_T = \mu_{\mathrm{Mn}} + \sum_X \mu_X.
$$

Here, $\mu_X(E_i)$ is the contribution to the total attenuation coefficient from the excitation of core electron X, and $\omega_X(E_f)$ is the probability of fluorescence at energy E_f resulting from electrons decaying to fill in the core hole left by X. E_i is an incident photon energy. $C = \eta(E_f)\Omega/4\pi$ is a constant given by the detector efficiency $\eta(E_f)$ and the solid angle Ω of the detector. α and β are the angles of incidence and emission, respectively, as measured from the sample surface.

A significant limitation of FY mode XAS arises from saturation effects [4], which distort peak intensities in the

measured spectra and make FY non-linear with respect to the absorption coefficient. Recently, Achkar *et al.* introduced an alternative method to measure the absorption spectra which is bulk-sensitive and does not suffer from saturation effects [5]. They used an energy-sensitive detector and measured the normal (non-resonant) x-ray emission spectrum (NXES) from a different element and absorption edge than the one probed resonantly with incident photons. The inverse of this NXES PFY is termed as the inverse partial fluorescence yield (IPFY), and is a function of the total x-ray absorption coefficient $\mu(E_i)$:

$$\mathrm{IPFY} = A(\mu(E_i) + B), \qquad (2)$$

where $A = 4\pi/\eta(E_f)\Omega\omega_Y(E_f)\mu_Y(E_i)$, and $B = \mu(E_f)\sin\alpha/\sin\beta$. Y denotes the core electron, for example, O $1s$. In Eqn. (2), the constant B is independent of E_i and A depends only weakly on E_i over a narrow energy range and can be treated approximately as constant. Therefore, IPFY is proportional to the XAS $\mu(E_i)$ plus an offset proportional to B.

In this paper, we show the different behaviors of La_2NiMnO_6 and $LiMnO_2$ at the Mn $2p$ absorption edges. One can see that the TFY makes peak structures in La_2NiMnO_6 and dip structures in $LiMnO_2$. This difference can be explained by the existence or absence of high-Z (Z: atomic number) elements such as La in this case. Then we show the usefulness of PFY and IPFY for the measurements of $LiMnO_2$. This technique should become an indispensable tool for the measurement of systems without high-Z elements such as Li-ion battery materials.

The thin film of La_2NiMnO_6 was fabricated on a $SrTiO_3$ substrate by the pulsed laser deposition technique, and the details were described in Refs. [6, 7]. The powder samples of $LiMnO_2$ were synthesized by the procedure described in Refs. [8, 9]. The thickness of the thin films used for this study was 50 nm. XAS experiments were performed at 11ID-1 (SGM) of the Canadian Light Source. The TEY spectra were measured using drain current. The TFY spectra were measured with a channel plate detector. The PFY spectra were measured using a silicon drift detector with an energy-resolution of ~ 120 eV. The resolution power ($E/\Delta E$) was set to 5000. All the spectra were measured at room temperature.

Figure 1 shows the energy resolved x-ray emission spectra of La_2NiMnO_6 (a) and $LiMnO_2$ (b) (normalized to the incident photon intensity) as the incident photon energy is scanned through the Mn $2p$ absorption edges. Emission spectra for several incident photon energies are shown in Fig. 2, and we can see x-ray emission peaks corresponding to the following two transitions Mn $L_{\alpha,\beta} \sim 640$ eV ($3d \rightarrow 2p$), and O $K_\alpha \sim 520$ eV ($2p \rightarrow 1s$). As expected, the Mn L emission increases as the incident photon energy passes through the Mn $2p$ edges. In contrast, the O K emission shows a small dip in the case of La_2NiMnO_6 (a), and a big dip in the case of $LiMnO_2$ (b).

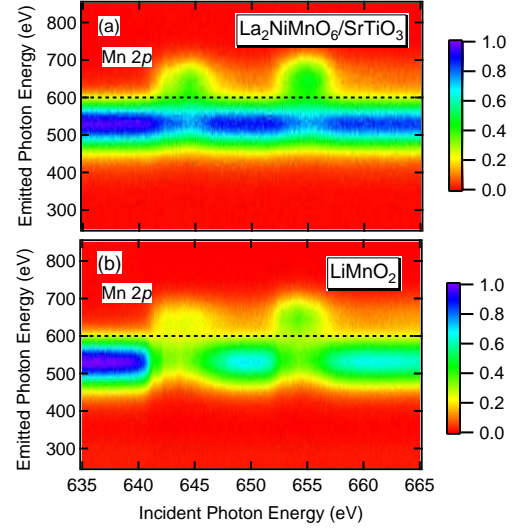FIG. 1: (Color online): Energy-sensitive fluorescence yield from La_2NiMnO_6 and $LiMnO_2$. In panel (a) [(b)], normalized PFY of La_2NiMnO_6 [$LiMnO_2$] as the incident photon energy is scanned through the Mn $2p$ edges.

The La in La_2NiMnO_6 has a much larger absorption cross section that the other elements in the material and dominates the total attenuation coefficient. Therefore, even at the Mn $2p$ edges, the attenuation length of the incident photons does not change significantly and so the intensity of the O K emission is not strongly reduced. When we measure the TFY from this sample, the absorption spectrum shows the expected positive structures, but they are slightly distorted by saturation effects, at the Mn $2p$ edges. The situation in $LiMnO_2$ is quite different. In this material, consisting of only low-Z elements, the penetration depth decreases greatly when exciting across the Mn $2p$ edge. This leads to a significant decrease in the O K_α emission that is larger in magnitude than the increase in Mn L_α emission. The resulting TFY spectrum exhibits dip structures as shown in Fig. 3. The dip structures are not apparent in the PFY. For PFY, a threshold photon energy of 600 eV can be used to separate the O K and Mn L emissions, as shown in Figs. 1 and 2. The PFY from the Mn L emission (> 600 eV) and the IPFY from the O K emission (< 600 eV) are shown in Fig. 3.

In the case of La_2NiMnO_6 (Fig. 3 (a)), the TFY shows less distortion by saturation effects than in $LiMnO_2$. The Mn L PFY displays stronger saturation effects, and the IPFY from O K emission shows increased noise because the intensity of O K emission does not change significantly at this edge, as shown in Fig. 2 (a). The IPFY of La_2NiMnO_6 also shows some distortion because the sample is only 50 nm thick. The IPFY method is based on the condition of total absorption, which, in this case, is not met at all photon energies. For $LiMnO_2$ (Fig. 3 (b)),
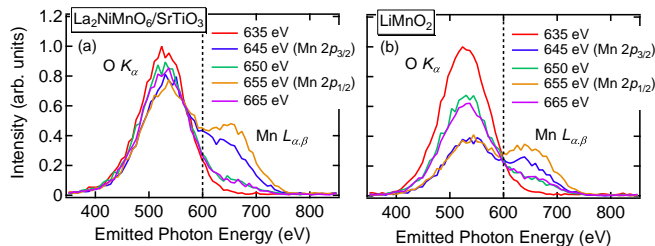
FIG. 2: (Color online): Emission spectra for several incident photon energies are shown for La_2NiMnO_6 (a) and $LiMnO_2$ (b). Emissions corresponding to the O K_α and Mn $L_{\alpha,\beta}$ transitions are observed.
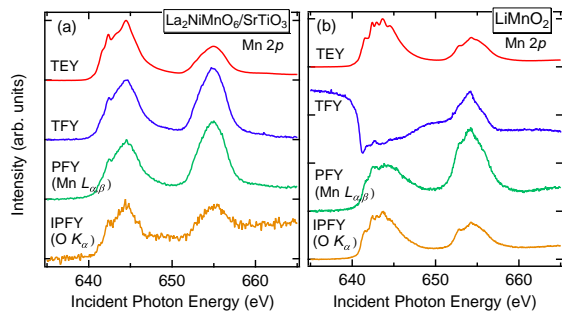

FIG. 3: (Color online): TEY, TFY, Mn L edge PFY and O K edge IPFY as a function of photon energy through the Mn $2p$ edges in the case of La_2NiMnO_6 (a) and $LiMnO_2$ (b).

the Mn L PFY has already been shown in Ref. [10], and is less significantly distorted by saturation effects. The IPFY derived from the O K emission does not show any saturation effects, unlike the PFY from Mn L emission, consistent with the report in Ref. [5]. This highlights that fact that TFY produces misleading spectra in many materials and that PFY is almost an indispensable tool to obtain bulk sensitive XAS spectra. Although reliable TEY spectra have also been measured on these materials, instances exist where surface contamination is significant or where the electronic states of the surface differ from the bulk [11, 12] and one must rely primarily on fluorescence detection. As demonstrated in this study, TFY is unsuitable for investigation of many Li-ion battery related materials, which is one of the most hotly debated topics in contemporary condensed-matter physics.

In conclusion, we have demonstrated the indispensability of the IPFY technique for XAS studies of low-Z battery related materials like $LiMnO_2$. While TFY can-

not be reliably applied to either $LiMnO_2$ or La_2NiMnO_6, there is significantly less distortion in the La_2NiMnO_6 which we attribute to the presence of the strongly absorbing La atoms which moderate the change in penetration depth when exciting across the Mn L edge. The PFY in both systems exhibits strong self-absorption effects. These effects are overcome by using the inverse of the O K PFY (IPFY), which is a good representation of the Mn XAS in $LiMnO_2$. As such low-Z systems are highly relevant battery materials, the IPFY technique will be a crucial tool for measuring accurate XAS spectra.

* Electronic address: wadati@ap.t.u-tokyo.ac.jp; URL: http://www.geocities.jp/qxbqd097/index2.htm
[1] F. de Groot and A. Kotani, *Core Level Spectroscopy of Solids* (CRC Press, New York, 2008).
[2] J. Stohr, *NEXAFS Spectroscopy* (Springer, New York, 1996).
[3] F. M. F. de Groot, J. Electron. Spectrosc. Relat. Phenom. **67**, 529 (1994).
[4] S. Eisebitt, T. Boske, J.-E. Rubensson, and W. Eberhardt, Phys. Rev. B **47**, 14103 (1993).
[5] A. J. Achkar, T. Z. Regier, H. Wadati, Y.-J. Kim, H. Zhang, and D. G. Hawthorn, Phys. Rev. B **83**, 081106 (2011).
[6] M. P. Singh, C. Grygiel, W. C. Sheets, P. Boullay, M. Hervieu, W. Prellier, B. Mercey, C. Simon, and B. Raveau, Appl. Phys. Lett. **91**, 012503 (2007).
[7] M. P. Singh, K. D. Truong, S. Jandl, and P. Fournier, Phys. Rev. B **79**, 224421 (2009).
[8] Z.-F. Huang, F. Du, C.-Z. Wang, D.-P. Wang, and G. Chen, Phys. Rev. B **75**, 054411 (2007).
[9] F. Du, Z.-F. Huang, C.-Z. Wang, X. Meng, G. Chen, Y. Chen, and S.-H. Feng, J. Appl. Phys. **102**, 113906 (2007).
[10] H. Wadati, D. G. Hawthorn, T. Z. Regier, G. Chen, T. Hitosugi, T. Mizokawa, A. Tanaka, and G. A. Sawatzky, Appl. Phys. Lett. **97**, 022106 (2010).
[11] L. A. Montoro, M. Abbate, E. C. Almeida, and J. M. Rosolen, Chem. Phys. Lett. **309**, 14 (1999).
[12] Y. Koyama, T. Mizoguchi, H. Ikeno, and I. Tanaka, J. Phys. Chem. B **109**, 10749 (2005).